NOTICE CONCERNING COPYRIGHT RESTRICTIONS

DOWNHOLE SEISMIC MONITORING OF AN ACID TREATMENT IN THE BEOWAWE GEOTHERMAL FIELD

Ravi Batra, James N. Albright,
and Christopher Bradley

Los Alamos National Laboratory

ABSTRACT

During the acid treatment of a subeconomic well at the Beowawe Geothermal Field, numerous seismic events were detected of which 22 could be located. The events occurred following a first stage of the acid treatment and generally define a trend paralleling the surface trace of the Malpais fault. No seismic signals were detected following a second stage of the acid treatment, despite the injection of almost twice as much additional fluid. It is postulated that the cause of seismic events following the first stage was due to shear failure of chemically weakened cemented fractures or joints in the reservoir. Presumably reservoir strain was sufficiently reduced to preclude further rock failure during the second day of treatment.

INTRODUCTION

The ROSSI 21-19 well at Chevron's Beowawe Geothermal Field has been a non-commercial producer even though it intersects a high temperature fluid zone. Pressure interference tests have established good hydraulic connectivity between all five wells in the reservoir and have also shown high area permeability within the reservoir. Limited productivity at ROSSI is thought to be due to near-wellbore restricted permeability. As part of the Department of Energy's eight-well stimulation program for geothermal reservoirs, Republic Geothermal, Inc. conducted the acid stimulation experiment at Beowawe. This experiment was a 60,000 gallon two-stage acid treatment designed to enhance productivity of the natural fractures and to remove drilling mud residue from the near-wellbore fractures around ROSSI. Los Alamos participated in this experiment to monitor the acid treatment process for evidence of reservoir strain release by locating the source of rock failure, as indicated by seismic signals, and to provide data on the direction of fluid movement in the reservoir during treatment.

The Beowawe Geothermal Field. The Beowawe Geothermal Field lies between a plateau of fractured Tertiary volcanics to the south, and the downfaulted Whirlwind Valley to the north (Figure 1). The area, a few miles southwest of the town of Beowawe and about 50 miles east of Battle Mountain, Nevada, has been the subject of several geological studies, most notably those of Smith (1983), Struhsacker (1980), Zoback (1979), and Garside and Schilling (1979). The location of the blowing wells, called The Geysers, is along the Malpais fault zone, an east-northeast striking Basin and Range normal fault. This fault developed after eruption of the basaltic andesites between late Miocene to Pliocene times and represents the more recent of two major episodes of faulting, controlling the location of the geothermal field. The older normal fault system, the Dunphy Pass fault zone, has a northwest trend, and terminates the geothermal system to the east. The sedimentary basement consists of Paleozoic carbonates overlain by the Ordovician Valmy formation. Highly permeable zones are probably located at several levels within the fractured Valmy formation under the Malpais Ridge/Whirlwind Valley area. The reservoir is perhaps in the lower Paleozoic carbonates at depths approaching 20,000 to

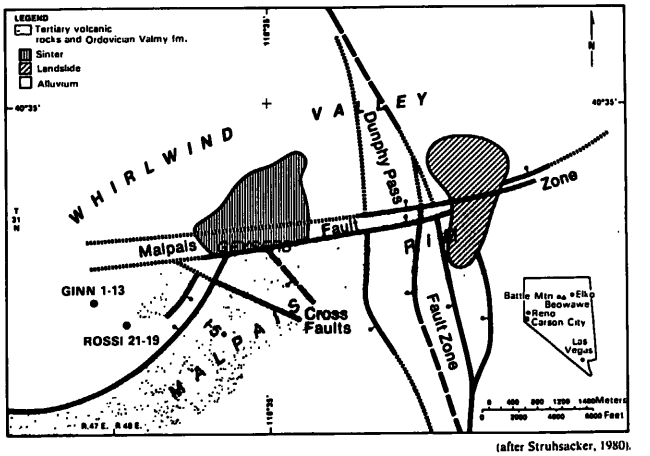

(after Struhsacker, 1980).

Figure 1. Location and generalized structure of the Beowawe area (after Struhsacker, 1980).

30,000 ft (Epperson, 1982), and with temperatures of 360-420°F (Republic Geothermal, Inc., 1983). The location of the treated well, ROSSI 21-19, is shown in Figure 1 at the base of the Malpais Rim. The position of GINN 1-13, used to monitor the activities at ROSSI, is also shown about 2000 ft to the northwest.

OBSERVATIONS

A triaxial geophone package, developed by Los Alamos for high-temperature use, was deployed in well GINN 1-13 about 2000 ft northwest of ROSSI 21-19. A single geophone was strapped to the wellhead casing. Analog output from the geophones was recorded on magnetic tape. This deployment occurred on August 21-22, 1983, during the two stages of acid treatment. No monitoring was conducted on August 20, 1983, when 1831 bbl of water were injected into the formation for the purpose of determining reservoir characteristics prior to the treatment.

August 21. The injection of acid and water at ROSSI 21-19 was confined to the slotted linear interval below 4369 ft. The ROSSI injection was monitored from several positions in GINN, commencing at 6500 ft, for about 30 min before acid injection (Figure 2). Monitoring continued at 6500 ft during acid injection (500 bbl at about 15 BPM rate) and, subsequently, during displacement of acid into the formation by flushing with 221 bbl of water. The tool was moved to 5500 ft just prior to injection of 2225 bbl of water at the same rate of about 15 BPM. Several microearthquake events were observed during the latter half of the water injection stage, especially subsequent to a sudden increase in surface treating pressure. A marked decrease in seismic signals was observed upon completion of water injection (Figure 2).

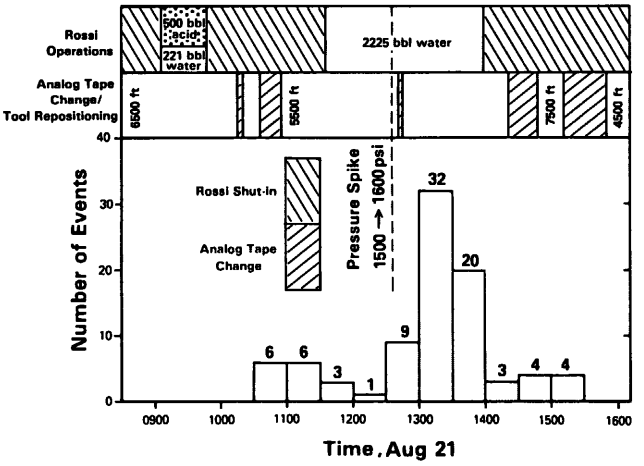

Figure 2. August 21 operations and monitoring schedule; event histogram.

August 22. Monitoring was resumed at 6500 ft just prior to injection of 982 bbl of an acid mixture consisting of 12% HCl and 3% HF, flushed with 297 bbl of water to displace acid into the formation. This process was interrupted for 20 min during the course of injection to repair an acid leak at the treating head and a hose leak on the blender discharge (Figure 3).

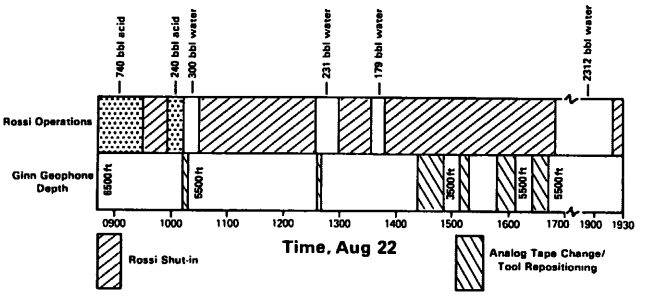

Figure 3. August 22 operations and monitoring schedule.

The tool was moved to 5500 ft prior to injection of water. The water injection stage was marked by several interruptions due to intermittent operations at ROSSI. Sustained water injection was resumed after a delay of at least 3 hours from the previous shut-down. Pumping continued uninterrupted for 2-1/2 hours at the rate of about 15 BPM. A total of 2312 bbl of water was injected during this stage. Seismic activity was not apparent on this second day of acid and water injection.

The observed seismicity during the first acid treatment on August 21 is in itself enigmatic because the stresses normally required to break rock, or to cause shear failure along preexisting fracture surfaces, were not achieved hydraulically. It is postulated that the seismic events may have resulted from the shear failure of fractures caused by chemical weakening of cementing material. However, if this hypothesis is valid, rock failure events should have been more pronounced on the following day, August 22, when a stronger acid mixture in larger volume was injected, unless reservoir stresses had been sufficiently released the previous day. However, if the observed microseismicity of the first day was indeed hydraulically induced, then lack of events the following day may be ascribed to the several interruptions in the injection process.

DATA ANALYSIS

Data Processing. All signals on magnetic-tape records of geophone output, having any portion of their coda exceeding 50 times background noise, were digitized into 800 msec,

2048-channel data blocks for processing. Digitized records were visually inspected for signal character and quality. Only seismic signals, showing characteristic P- and S-wave arrival and decay, were further processed. Figure 4 shows one such signal as detected along X, Y, and Z geophone axes. P-wave and S-wave arrivals are strongest on the Y and Z geophone outputs, respectively. The absence of a clearly defined S-wave arrival on the horizontal geophones indicates that S-wave is predominantly vertically polarized. Figure 5 gives the composite power spectrum of the geophone output shown in Figure 4. Signal power is generally restricted to the 10-140 Hz frequency band.

The origins of seismic signals, hence the locations of the rock failure during the acid treatment, were determined using (i) the time difference between S- and P-wave arrivals, and (ii) the average polarization of particle motion at the geophone sonde during the time represented in the P-wave coda. If the propagation velocity of P- and S-waves is known or can be estimated, then the distance to the signal source can be calculated using (i). The direction to the signal source is the direction of particle motion polarization measured in (ii). In the absence of knowledge of generalized velocity structure between signal source and detector, the distance and direction to the origin of the seismic signal indicate the most probable location of rock failure.

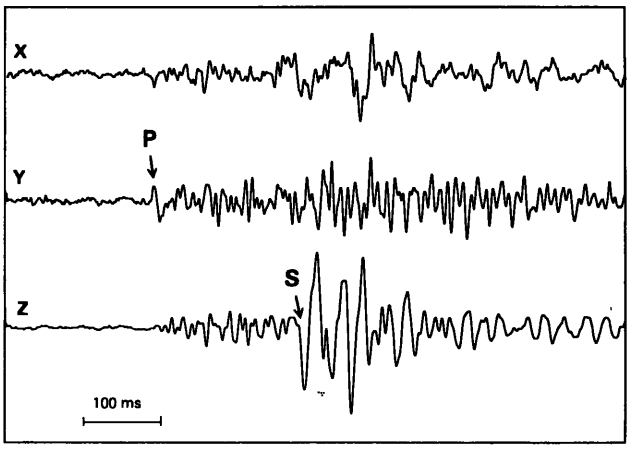

Figure 4. Typical rock failure signal.

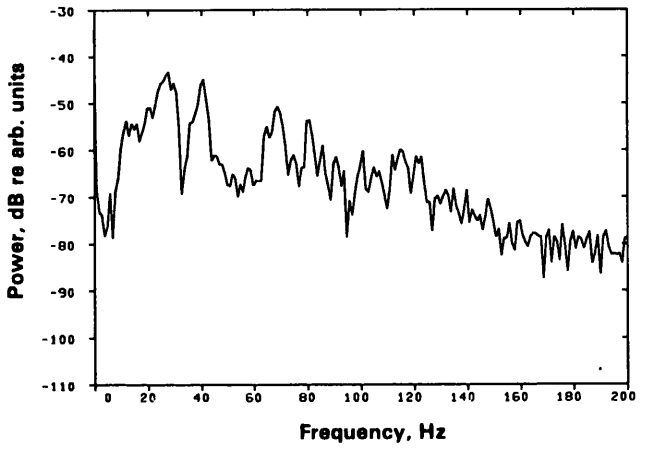

Figure 5. Composite power spectrum of signal given in Figure 3.

S-P Delay Times. The seismic velocities used for locating these events with respect to the GINN well were obtained from the pseudosonic geophone survey in GINN run by Chevron Resources in 1982. Over the interval of interest (i.e., a few hundred feet above and below the injection interval), P-wave seismic velocities are of the order of 15,500 ft/sec. Assuming a normal Poisson's Ratio of .25, the shear wave velocity would be 8960 ft/sec. The measured time difference between P- and S-wave arrivals were then used to compute the distance to the site of rock failure from the GINN well.

P-wave Polarization. Based on the design of the acid treatment, the vertical extent of the reservoir to be affected was roughly 300 ft centered about 5500 ft in ROSSI. Thus, rock failure signals that were detected at the same depth in GINN gave rise to signals impinging within 4° of the plane defined by the horizontal geophone axes. In Figure 4, the apparent delay in P-wave onset on the Z-geophone confirms that this indeed was so. Because of the low angle we can ignore Z-geophone output in computations of polarization with little loss in accuracy.

Average polarization in the P-wave coda was calculated as follows. If $X_p(t)$ and $Y_p(t)$ represent P-wave coda as measured along the X and Y directions, respectively, then Θ_{xy}, the average polarization angle with respect to the X-geophone direction is:

$$\tan \Theta_{xy} = \frac{\Sigma X_p(n\Delta t) \cdot \Sigma Y_p(n\Delta t)}{\Sigma X_p(n\Delta t) \cdot \Sigma X_p(n\Delta t)}$$

Previous investigators (Albright and Pearson, 1982) who have used polarization for mapping purposes have restricted $n\Delta t$ to the period of the first cycle, or a fraction thereof, of the P-wave coda. Stated differently, the polarization direction in these studies was determined from the first motion sensed at the geophone. This approach fails when the S/N of the first motion is poor and not statistically compensated for by a commensurately large number of signals available for processing. Because the Beowawe data consist of a small number of signals, with relatively poor S/N during first motion (2-10 on the horizontal components), the coda method was

elected for use. To the best of our knowledge, a satisfactorily complete theoretical and/or empirical comparison of the relative merits of first-motion and coda polarization methods has not been undertaken. Such a comparative study is, however, outside the scope of the Beowawe measurements. The use of the coda method, however untested, has presented us with potentially significant and intriguing results, which we summarize below.

Geophone Package Orientation. The geographic orientation of geophone axes is customarily determined from a measurement of the attitude of the borehole package and the well deviation at the monitoring depth. Attitude is obtained through interrogation of axial inclinometers housed in the package. Because neither multishot nor gyroscopic deviation surveys are available for GINN, an attempt was made to orient the downhole package using dynamite as a source of seismic energy. Two shots placed on the pediment of the Malpais Range to 2000 ft south of ROSSI, in line with GINN, failed to produce a detectable signal at the monitoring depth of 5500 ft.

RESULTS

Rock Failure Map. Figure 6 shows the locations of rock failure that could be determined using P-wave coda polarization measurements projected onto the XY horizontal plane at the depth of fluid injection. These events are grouped in the distance range (1580-2110 ft) from the GINN well, indicating that they occur close to the ROSSI injection well. The occurrence of these events is based on the assumption that rock failure is related to the injection process and perhaps caused by fluid gaining access to a system of conjugate fractures. This is possible since, as mentioned earlier, stresses required to break rock were not achieved hydraulically.

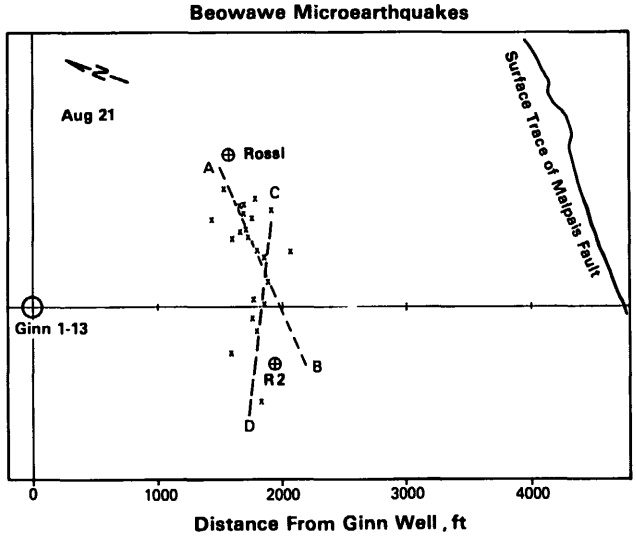

Figure 6. Beowawe rock failure locations (geophone orientation assumed).

Although not indicated in Figure 6, the locations of rock failure have a random spatial distribution with respect to pumping time. In other words the distribution of these events about the ROSSI well do not fall into any pattern during the course of fluid injection. However, 80% of the events appear to occur along two generally linear trends, AB and CD (Figure 6). We have used the AB trend to orient the rock failure map on the assumption that it lies parallel to the surface trace of the Malpais fault. If the trend of this prominent fault at depth is assumed to be along AB, then the ROSSI well projects to the location indicated, generally north and asymmetric to the mapped rock failure locations. If, instead, CD is assumed to be parallel to the Malpais fault, then the ROSSI well projects approximately 20° to the south with respect to GINN, again asymmetric to mapped locations. The ROSSI well may indeed be anywhere in between, perhaps even in the middle of the cluster of events. Lack of orientation of the geophone package precludes an exact location for ROSSI, with respect to the location of events.

Recurrence Relation. Figure 7 gives the recurrence relation for all events observed though not necessarily located on August 21, showing the cumulative number of events vs magnitude. The slope, or 'b' value, of such plots are thought to be characteristic of different seismic environments. The calculated magnitudes are based on event 'coda length', normalized to the northern New Mexico standard. This computation is based on the formula:

$$M = 2.79 \log(T) - 3.63,$$

where M = magnitude and T = coda length.

The 'b' value plot in Figure 7 shows that the detection threshold is around M = 4. A 'b' value of 0.68 is comparable to microearthquake activity associated with wellbore treatment in other geothermal areas.

Distribution of Events with Magnitude. Figure 8 is a histogram depicting the distribution of events with magnitude. It is worth noting that magnitudes so determined are relative magnitudes and that substantial uncertainties may exist in the determination. This is inherent in the difficulty in determining event coda, as well as the lack of a local "standard" for converting 'coda lengths' to magnitude. Similar arguments may be advanced for the uncertainties in the recurrence relationships ('b' values), including the possibility of omitting some seismic signals and counting others that are non-seismic. The latter argument is especially valid for the smaller magnitudes, in this case below M = -4.

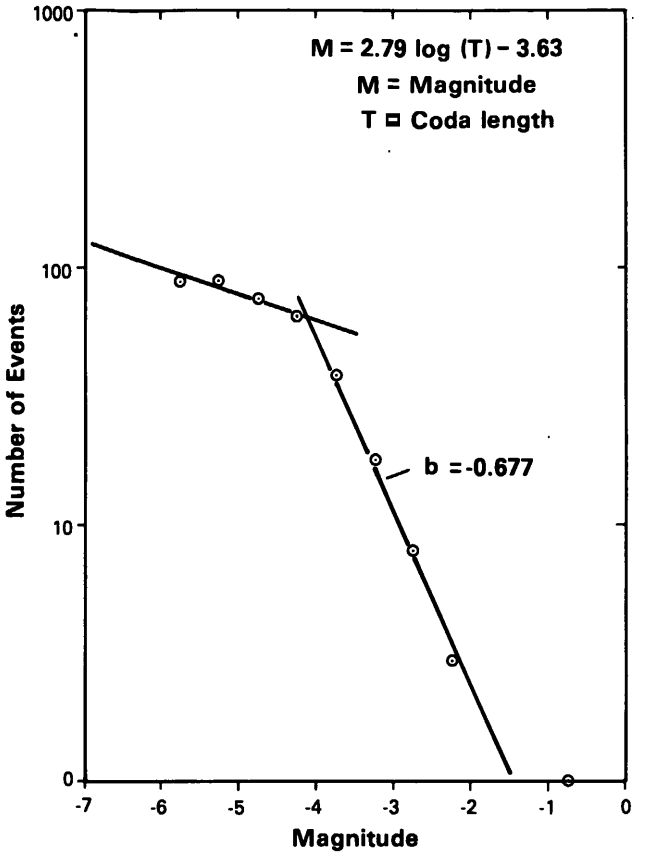

Figure 7. Recurrence relation for August 21 treatment.

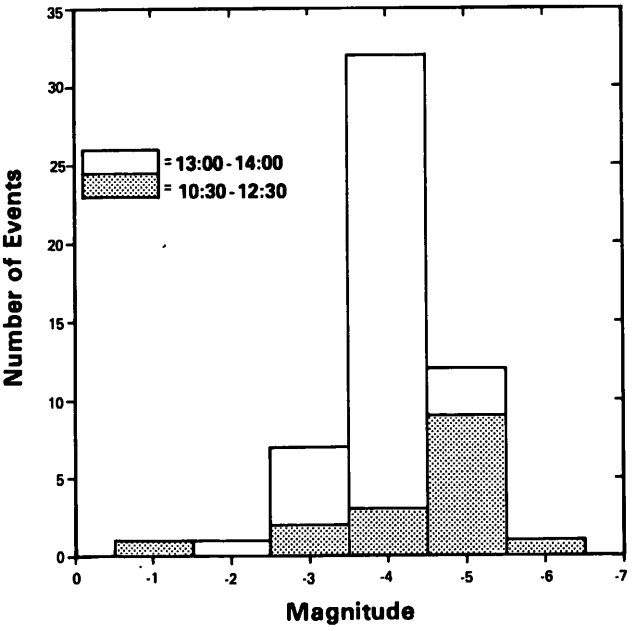

Figure 8. Rock failure event histogram for August 21.

SUMMARY

Downhole seismic monitoring provided an effective way to detect rock failure during reservoir stimulation experiments at Beowawe. Discrete seismic signals were detected that may be attributed to shear failure of fractures or joints due to chemical weakening by acid penetration, following the first day of treatment. Lack of similar events on the next day of treatment suggests significant reservoir strain release on the previous day. Rock failure events occur close to the injection well and define a generally linear trend, largely paralleling the surface trace of the Malpais fault. Signal power is generally restricted to the 10-140 Hz frequency band. The detection threshold for these events was about M = -4, and gave a 'b' value of 0.68.

ACKNOWLEDGMENT

The authors wish to thank Will Dasie, Chevron Resources, Co., for critically reviewing this manuscript and offering valuable suggestions. We are grateful to Everett Horton for supervising the data acquisition under trying conditions.

REFERENCES

Albright, James N., and C. F. Pearson, 1982, Acoustic Emission as a Tool for Hydraulic Fracture Location: Experience at the Fenton Hill Hot Dry Rock Site, Soc. of Pet. Engrs. Journal, August 1982, p. 523-530.

Garside, L. J., and J. H. Schilling, 1979, Thermal Waters of Nevada, Nev. Bur. of Mines and Geol. Bull. 91, p. 163.

Republic Geothermal, Inc., 1983, Proposal for Producing Well Chemical Stimulation Treatment, Beowawe Geothermal Field, Experiment No. 8, prepared for the U.S. Dept. of Energy, Geothermal and Hydropower Technologies Div.

Smith, C., 1983, Thermal Hydrology and Heat Flow of the Beowawe Geothermal Area, Nevada, Geophysics, Vol. 48, No. 5, p. 618.

Struhsacker, E. M., 1980, The Geology of the Beowawe Geothermal System, Eureka and Lander Counties, Nevada, DOE/ID/12079-7, U.S. Dept. of Commerce, NTIS, Springfield, VA.

Zoback, M. L., 1979, Geologic and Geophysical Investigation of the Beowawe Geothermal Area, North-Central Nevada, Stanford Univ., Sch. of Earth Sciences, Geological Sciences Series, Vol. XVI.